

*Розглянуто теплофізичну модель сотових конструкцій з дефектом типу непроклей. Запропоновано метод зниження перешийку, характерних для поверхні сотових конструкцій, за рахунок оптимізації режиму контролю теплової дефектоскопії та подальшої фільтрації перешийку, викликаних неоднорідною структурою зразка. Запропонований метод зменшення перешийку включає в себе дві процедури: процедуру запобігання зростання перешийку та процедуру подальшого зменшення цих перешийку*

*Ключові слова: сотова конструкція, тепла дефектоскопія, випромінювальна здатність, непроклей*

*Рассмотрена теплофизическая модель сотовых конструкций с дефектом типа непроклей. На ее основе исследован процесс дефектоскопии сотовых конструкций. Предложен метод снижения помех, характерных для поверхности сотовых конструкций, за счет оптимизации режима контроля тепловой дефектоскопии и дальнейшей фильтрации помех, вызванных неоднородной структурой образца: предложенный метод подавления помех включает в себя две процедуры. Процедуру предотвращения роста помехи и процедуру последующего ее подавления*

*Ключевые слова: сотовая конструкция, тепловая дефектоскопия, излучательная способность, непроклеи*

UDC 621.396.6

DOI: 10.15587/1729-4061.2016.79563

# OPTIMIZATION OF THE PROCEDURE OF THERMAL FLAW DETECTION OF THE HONEYCOMB CONSTRUCTIONS BY IMPROVING THE ACCURACY OF INTERFERENCE FUNCTION

**V. Storozhenko**

Doctor of Technical Sciences, Professor\*

E-mail: d\_ph@nure.ua

**A. Myagkiy**

Postgraduate student\*

E-mail: shoor\_80@mail.ru

**R. Orej**

PhD, Associate Professor\*

E-mail: oryol\_rp@yahoo.com

\*Department of physics

Kharkiv National University of Radio Electronics  
Nauki ave., 14, Kharkiv, Ukraine, 61166

## 1. Introduction

Honeycomb constructions are the most widely used materials in contemporary aviation and space technology. They are the basis for the housings of practically all products of this sector, where reliability of all parts should meet the increased requirements. Special attention is paid to the quality of composite materials and to the absence of defects such as the places of adhesion failure (exfoliation) between the skin and the honeycomb filler [1].

It is known that to detect the defects of this type, it is promising to apply thermal flaw detection [2], which combines high sensitivity to detection of flaws of this kind with a high rate of control [3] (with the use of a thermal imaging system as a recorder).

However, in comparison with other methods of nondestructive control, the use of thermal control is connected with a number of factors, which complicate its application. The main problems of application of thermal nondestructive control (TNC) are both the existence of a large quantity of noises and interferences of different nature and the fact that the thermal flaw detection is conducted, as a rule, not under optimum regimes, which substantially worsens detectability

of flaws and limits reliability of control results. As a result, a wide range of objects (first of all, composition structures), for the flaw detection of which the thermal method is the most promising, is not controlled efficiently enough, which does not ensure necessary quality and reliability in operation.

Therefore, increase in the efficiency and reliability of thermal flaw detection, based on in-depth analysis of the processes of detecting defects and development of the principles of optimization of both the procedure of control and subsequent processing of the obtained information, is an important and relevant task.

## 2. Literature review and problem statement

The main task of thermal control is establishment of correlation between a registered temperature field of an object of control and parameters of internal structure of the object, which is revealed owing to uneven propagation of heat flow [4]. Heat propagation has the form of heat exchange between the bodies, which have different temperatures. There are three different ways of heat transfer: thermal conductivity, convection and radiation. In practice, all three are applicable, but to

a different degree, which is determined by specific initial and boundary conditions [5]. To establish a correlation between a registered temperature field of the object of control and parameters of internal structure, an appropriate thermophysical model is created [6]. The use of the selected thermophysical model together with experimental data makes it possible to establish the required parameters of a flaw [7], namely, its dimensions, disclosure and depth of bedding.

But the use of the procedure of thermal flaw detection is complicated by existence of the noises, which by magnitude can be compared with a useful signal [8] and essentially complicate the procedure of TNC. In our case, there are four kinds of noises: externally produced, hardware, internally produced interference and random noise [9].

An externally produced interference is created by the thermal flow of the environment, either reflected from a control object or falling directly into the entrance pupil of the thermal imaging system. The sources of this noise are heaters, the Sun, air stoves, lamps of electrical illumination, etc. Direct radiation is usually removed with the use of blends, screens and filters [10]; a similar method is rather effective under laboratory conditions, but is not always implemented under industrial conditions. Radiation in the infrared range, caused by reflection from the object of control of the working parts of the plant is more difficult to remove [11]. In the active TC, the main source of external noise is a heater [12] and inhomogeneity of radiation capacity of the object of control (OC) [13]. The heterogeneity of thermal field of a heater is, as a rule, compensated for by additional study of the heater itself [12]; however, this method is not applicable if a heater is located inside the unit or a working substance serves as a heater. Reduction in the noise influence, caused by inhomogeneity of radiation ability of OC, is achieved due to the optimization of the TNC procedure by the signal/noise criterion [13]; the method is rather efficient if there are no other multiplicative noises; besides, this method ignores additive noises.

There is a whole range of methods used for the suppression of these interferences but they have a number of drawbacks or are not applicable under certain conditions. Thus, the «heat wave» method effectively suppresses interferences, caused by internal inhomogeneity of the sample, and restores the profile of a layer [14], but it requires the end heating, which it is not possible for extended objects. The method «Shape from heating» works well on cylindrical objects [15], but it is not applicable for the objects of another form because of specific character of its design. The joint use of the methods «SUSAN» and «Roberts» [16] filters the noise, caused by a reflected signal, but it requires the use of additional data, obtained from the same position, which is feasible only at the thermal imaging systems with aligned lens.

It follows from this that the existing methods are not optimum for the suppression of the complex of interferences, characteristic for the tested sample, or require additional studies. For this reason, the TNC accuracy is decreased and its automation becomes difficult.

In all the methods described above, each interference is examined separately, without taking into account their mutual effect.

### 3. Aim and objectives of the study

The purpose of the work is the increase in sensitivity and reliability of thermal flaw detection by suppression of inter-

ferences and noises by optimization of the control procedure with subsequent processing of the obtained results based on the example of controlling the honeycomb structures.

To achieve the aim, the following tasks were set:

- to analyze factors, which limit sensitivity and reliability of TFD, as well as the existing methods of dealing with them;

- to build up a thermophysical model, adequate to real objects and to the conditions for conducting TFD, to explore basic flaw detection processes and to establish optimum regimes of conducting TFD by optimization criterion – maximization of ratio “signal/interference” on the basis of the created thermophysical model;

- to implement the method of optimization of TFD procedure by the criterion of maximum of “signal/interference” in the form of procedure allowing calculating optimum control modes, as well as processing the obtained information by decreasing the interference level.

## 4. Theoretical studies

### 4.1. Calculation by the thermophysical model

A multilayer plate was chosen as a thermophysical model of the object of control (OC), which adequately reflects actual design of the honeycomb structure, which consists of carbon plastic skin, between two layers of which the honeycombed plastic is placed (Fig. 1).

Inhomogeneities such as the adhesion failure between the skin and the honeycombed plastic, simulated by the air layer, and an interference of the “inhomogeneity of glue layer” type, simulated by inclusion of a foreign material in the honeycombed plastic, are also given in Fig. 1. Cylindrical coordinate system is used for the calculations by the thermophysical model:  $r$  is the radial coordinate;  $z$  is the vertical coordinate,  $\varphi$  is the angular coordinate.

A number of interferences, such as nonuniformity of radiation capacity of the sample’s surface and the “edge effect” are simulated separately [3, 5].

For efficient interference suppression, they were divided into two groups, the first one, with regard to its properties [3, 5], is suppressed by optimization of the control regime, and the second one – by subsequent mathematical processing of the obtained thermograms, by sequential filtration.

Calculations by the thermo-physical model were performed by two methods and were also compared to the data, obtained as a result of the experiment, on several different samples.

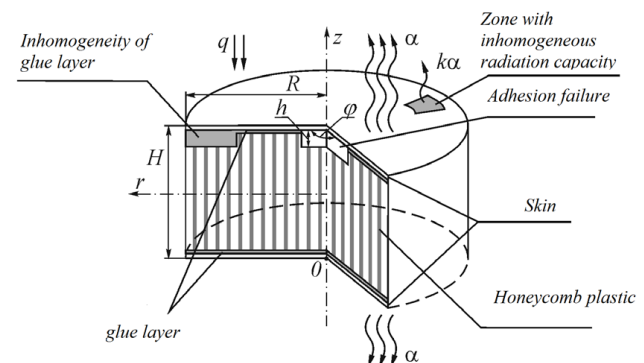


Fig. 1. Object of control:  $R$  – OC radius;  $H$  – OC thickness;  $q$  – power of heating;  $\alpha$  – coefficient of surface heat-transfer

In the selected thermophysical model, the layer of honeycomb plastic (Fig. 2) was substituted by the equivalent layer with thermophysical characteristics  $c', \rho', \lambda'$ , described by the following equations.

$$c' = \langle c \rangle = \frac{V_1 C_1 + V_2 C_2}{V_1 + V_2}, \tag{1}$$

$$\rho' = \langle \rho \rangle = \frac{V_1 \rho_1 + V_2 \rho_2}{V_1 + V_2}, \tag{2}$$

$$\lambda' = \langle \lambda \rangle = \frac{V_1 \lambda_1 + V_2 \lambda_2}{V_1 + V_2}, \tag{3}$$

where  $V_1$  is the polymer volume;  $V_2$  is the air volume;  $c', \rho', \lambda'$  are the thermophysical characteristics (TPC) of equivalent layer;  $c_1, \rho_1, \lambda_1$  are the thermophysical characteristics of polymer;  $c_2, \rho_2, \lambda_2$  are the thermophysical characteristics of air.

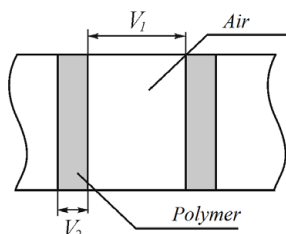


Fig. 2. Scheme of honeycomb plastic layers

Thermophysical model (Fig. 1) was built by the given geometric model and was set by boundary conditions (4)–(6), reflecting actual conditions for conducting TFD [1], that is, heating OC by external heat source, heat exchange with the environment with a coefficient.

On the external OC surfaces, the boundary conditions of the 2<sup>nd</sup> and 3<sup>rd</sup> types are satisfied:

– for  $z=H$

$$\left( \lambda(\vec{r}, t) \frac{\partial T(\vec{r}, t)}{\partial n} \right) \Big|_S = \alpha \left( T(\vec{r}, t) \Big|_S - T_{\text{среды}} \right) - q(\vec{r}, t), \tag{4}$$

– for  $z=0$

$$-\lambda(\vec{r}, t) \frac{\partial T(\vec{r}, t)}{\partial n} \Big|_S = -\alpha \left( T(\vec{r}, t) \Big|_S - T_{\text{среды}} \right), \tag{5}$$

– for  $z=h$

$$-\lambda_1(\vec{r}, T, t) \left( \frac{\partial T_1(\vec{r}, t)}{\partial n} \right) \Big|_S = -\lambda_2(\vec{r}, T, t) \left( \frac{\partial T_2(\vec{r}, t)}{\partial n} \right) \Big|_S, \tag{6}$$

where  $T(x, y, \tau)$  is the coordinate-time function of temperature;  $\lambda$  is the coefficient of thermal conductivity of the OC materials;  $q$  is the density of heat flow, from the external source (heater);  $\rho$  is the density of the OC materials.

A special feature of this model, in contrast to a number of the known models [1, 2], is the simultaneous use of both heat release from the heated surface and the calculation of thermal conductivity through the flaw  $\alpha$  (air).

Analysis of the constructed thermophysical model is conducted by the method of solution of differential equa-

tion of non-stationary thermal conductivity, recorded for the selected cylindrical coordinate system:

$$\text{div}(\lambda(\vec{r}, t) \nabla T(\vec{r}, t)) + q(\vec{r}, t) = c\rho \frac{\partial T(\vec{r}, t)}{\partial t}, \tag{7}$$

where  $c$  is the specific heat capacity of the OC materials;  $\rho$  is the density.

To solve equation (7), the numerical (grid) method of finite differences and the finite elements method were used.

For its implementation, the “TermoPro\_2009S” software package [17], earlier developed by Authors, was used, it enabled calculation of the optimum modes of controlling laminar structures, to simulate the signal and interference on the OC surface. The reference data on one of the varieties of honeycomb structures were used as numerical material (Table 1).

Table 1

Characteristics of OC materials

Characteristics of materials	Carbon plastic of skin	Polymeric honeycomb filler
Heat conductivity (Wt/mK)	0,3–0,9	0,065
Blackness degree	0,8–0,82	–
Thickness (mm)	0,8	28
Cell size (mm)	–	2,5

Numerical parameters of the simulated flaw (air layer) were selected as follows:  $h=0,8$  (which corresponds to thickness of the skin), disclosure (thickness)  $\delta=0,2$  mm (corresponds to thickness of the glue layer), transverse size  $l=5$  mm (corresponds to size of two cells).

Analysis of the developed thermophysical model was carried out employing the procedure, embedded in the above indicated software package, namely: equation (7) with boundary conditions (4)–(6) was solved, and the required value was the temperature contrast  $\Delta T$  on the OC surface above the flaw bedding place [1]. In this case, parameters of the mode of conducting TFD varied: density of heat flow  $q$ , duration of heating the OC surface  $\tau_q$ , the time lag of  $\tau_q$  (time interval between the end of heating and registration of temperature field). In this case, maximum temperature of heating the OC surface was limited by the value of 100 °C (for avoiding destruction of the material).

From the obtained array of values, the optimum TFD regime was determined (by the criterion  $\Delta T \rightarrow \Delta T_{\text{max}}$ ), TFD regime is given in Table 2.

Table 2

Results of calculating optimum TFD regime

$q, \text{kWt/m}^2$	$\tau_q, \text{s}$	$\tau_l, \text{s}$	$\Delta T, \text{°C}$
28	15	3,3	1,73

Let us note that in this case the mode is not final since optimization by the criterion “signal/interference” was not carried out yet.

**4. 2. Decrease in the influence of interferences from the first group on the determining of optimum control mode**

The main task of this part of the study is analysis of the influence of nonuniformity of the OC radiation capacity  $\epsilon$  on the flaw detection.

To solve this problem, the change in the heating power  $q$  was used, equivalent to the change  $\varepsilon$ . Actually, if, for example, in some section of the surface of the control object  $\varepsilon$  deviates to the larger side, then the heating of this section, that is,  $T_{max}$ , will be larger.

Results of this simulation are given in Fig. 3, where the development of the surface temperature for two cases over time is presented: Fig. 3, *a* is the faultless model with deviation by  $\varepsilon$ ; Fig. 3, *b* – model with a flaw.

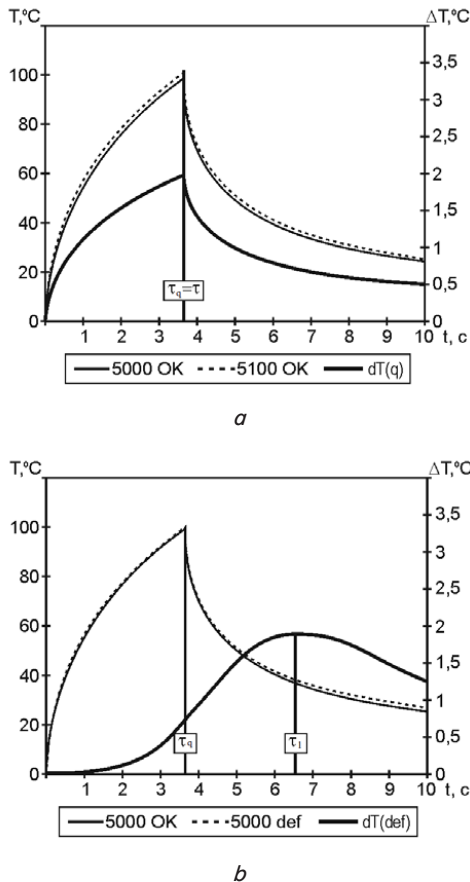


Fig. 3. Development of surface temperature over time for: *a* – faultless model with deviation by  $\varepsilon$ ; *b* – model with a flaw

Comparison of the presented dependencies demonstrates that the moments of time, which correspond to the maximum values of the interference  $\Delta T_\varepsilon$  and the useful signal  $\Delta T_{def}$ , do not coincide: the signal from the interference reaches a maximum immediately after heating, and the useful signal – with a certain time lag  $\tau_1$ .

This fact opens up a possibility to maximize the ratio signal/noise (that is,  $\Delta T_{def}/\Delta T_\varepsilon$ ) via selection of the optimum time of registration of temperature field on the surface of the control object.

This conclusion is also valid for the interferences of another type – uneven heating of the OC surface, that is, fluctuation  $q$ .

Thus, let us form “interference function”  $U(x, y, \tau)$  that considers additive and multiplicative interferences (8) for improving the accuracy of calculation of the optimum control mode [4, 7].

$$U(x, y, \tau) = \tilde{M}T(x, y, \tau) + \tilde{A}, \tag{8}$$

where  $M$  is the multiplicative interference;  $A$  is the additive interference;  $T(x, y, \tau)$  is the distribution of the calculated temperature field of OC.

Thus, obtaining the maximum value of criterion  $\Delta T_{def}/\Delta U$ , instead of the criterion  $\Delta T_{def}/\Delta T_\varepsilon$ , we obtain a more accurate value of registration time for the optimum control mode.

In particular, according to data in Fig. 3, *b*, when selecting the time lag  $\tau_1=6,35$  s, the signal/noise ratio equals 0,4, and at  $\tau_1=6,65$  s, this ratio reaches 2,6, that is, it is 6,5 times larger.

The developed model makes it possible not only to optimize control mode in terms of the indicated criterion, but also to determine the response threshold of the method.

### 5. Experimental studies of the honeycomb construction

To verify the results, obtained theoretically, we carried out experiments using the sample of a honeycomb construction, the parameters of which are given in Table 1. The sample contained two identified flaws with sizes given in Fig. 4. In the upper right and the lower left lower area of OC: 1)  $40 \times 70$  (mm); 2)  $20 \times 80$  (mm).

The rest of the parameters corresponded to the calculated ones: depth  $h=0.8$  mm, disclosure  $\delta=0,2$  mm.



Fig. 4. Scheme of location of flaws in the sample

To conduct the experiments, we used the thermal imaging system IRTIS-200, the area heater of radiation type, created by Authors, which is controlled by the timer (heating area of the heater, that is, frame, is  $15 \times 15$  cm, nonuniformity of heating by the frame field is 12 %).

To check the optimality of the calculated control mode, a series of thermograms was obtained: in the optimum control regime, before and after it. Two of them are given for illustration in Fig. 5.

It can be seen from the thermograms that in the optimum regime, the thermal contrast, caused by the flaw, is substantially higher ( $\Delta T=1,53$  °C) than in the non-optimal regime ( $\Delta T=0,54$  °C). The difference between the experimentally obtained value ( $\Delta T=1,53$  °C) and the calculated one ( $\Delta T=1,73$  °C) is within error limits. In this case, the experimentally obtained value  $\Delta T(1,53)$  is very close to the calculated one (1,73).

However, in this case, together with the useful signal on the thermograms, there are some temperature contrasts,

caused by interferences (noise signal). The magnitudes of temperature contrasts, caused by interferences, are comparable by magnitude to the useful signal ( $\Delta T_{def}=1,36\text{ }^{\circ}\text{C}$ ). If we use an amplitude sign for identification, the reliability of their detection will be low.

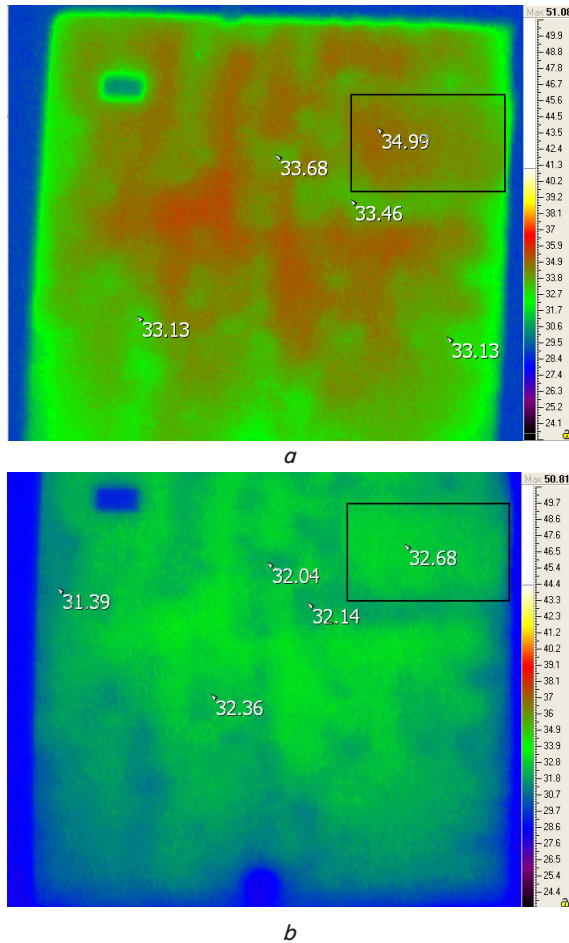


Fig. 5. Thermograms of control object: *a* – optimum regime; *b* – arbitrary regime

## 6. Processing the results of TDF for interference suppression

### 6. 1. Interference suppression, caused by heating nonuniformity

To compensate for the nonuniformity of heating, it is proposed to use normalization of inverse distribution function  $q(x, y)$  by the frame area. For this purpose, it is necessary to experimentally obtain distribution function  $q(x, y)$ . Then we should use computer processing of thermograms on the basis of equation (9), as a result of which, the nonuniformity of heating is decreased to 4–6 % (Fig. 6).

$$F' = \frac{q_{max}}{q} F, \tag{9}$$

where  $F$  is the matrix of values of thermogram temperatures;  $F'$  is the matrix of corrected values  $T$ ;  $q$  is the matrix of values of heating power;  $q_{max}$  is the maximum element  $q$ .

The thermogram, presented in Fig. 6, displays that the signal became more powerful but the flaw still cannot be unambiguously identified with regard to the fact that the thermogram still has interferences of the second group, which cannot be removed by optimization of the control regime, namely, the interference, caused by the nonuniformity of the glue layer.

biguously identified with regard to the fact that the thermogram still has interferences of the second group, which cannot be removed by optimization of the control regime, namely, the interference, caused by the nonuniformity of the glue layer.

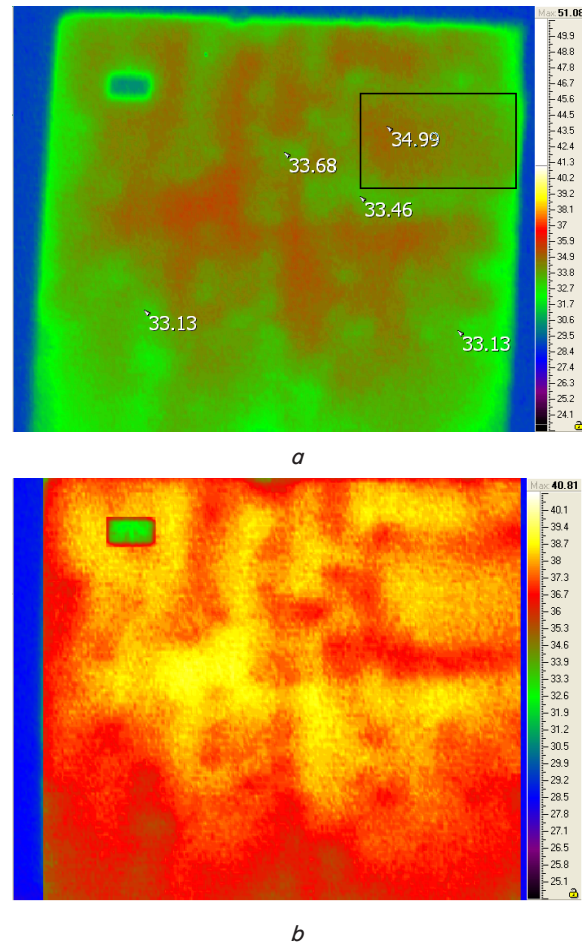


Fig. 6. Thermograms of the control object: *a* – before correction; *b* – after its execution

### 6. 2. Removing the interference, caused by inhomogeneity of the glue layer

The inhomogeneity of the glue layer is equivalent to the change in thermal resistance and leads to the occurrence of temperature contrasts on the OC surface. Analysis of the obtained experimental data revealed that these contrasts are different from the useful signal ( $\Delta T$  caused by a flaw) by the time dependence  $\Delta T(\tau)$ . This fact was used for constructing the method of suppression of this interference by a computer processing of thermograms using construction  $\partial T(x)/\partial \tau$  from  $x$  for the interference (Fig. 7), and for the underlying flaw (Fig. 8).

As it can be seen from Fig. 7, 8, these functions are easily distinguished, which became the basis of the method.

The essence of the method lies in the calculation of a two-dimensional matrix, the elements of which are the corresponding partial derivatives of time (10):

$$\hat{F}_{ij} = \frac{\partial F'_{ij}(x, y, u)}{\partial t}, \tag{10}$$

where  $F'_{ij}$  is the matrix element of corrected temperatures;  $i, j$  are the integral numbers, the number of the corresponding pixel along  $x$  and  $y$ ;  $F_{ij}$  is the characteristic matrix.

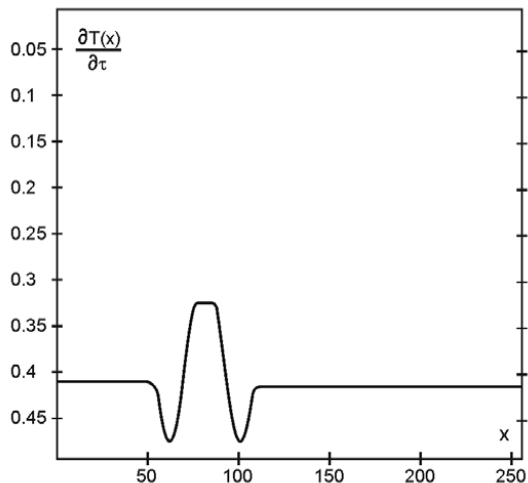


Fig. 7. Distribution of partial derivative of time along the x coordinate for interference

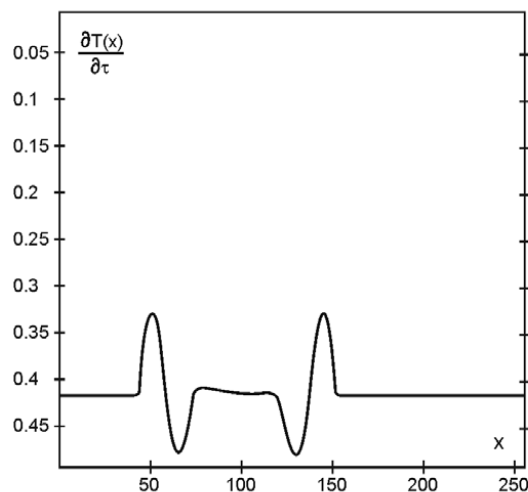


Fig. 8. Distribution of partial derivative of time along the x coordinate for a flaw

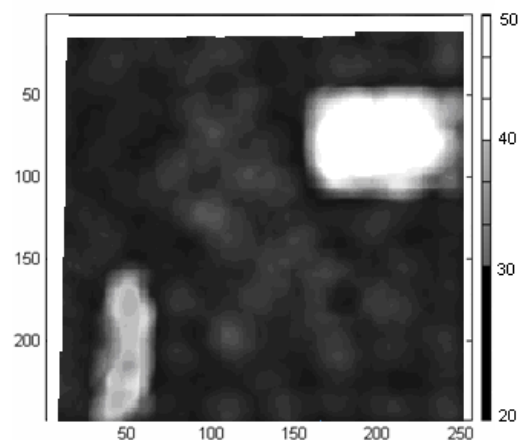


Fig. 9. Final view of thermogram after processing

After deciphering  $F_{i,j}$ , using dependencies, given in Fig. 7, 8, we obtain the final view of the thermogram after processing (Fig. 9). Comparison of this thermogram with the original one (Fig. 3, a) confirms the fact that the reliability of flaw detection substantially increased after processing.

This creates all prerequisites in order to proceed, under industrial conditions, from the visual method of flaw identification to the automated method, based on the appropriate technical tools.

### 7. Analysis of the obtained results

We proposed methods for dealing with interferences, caused by the nonuniformity of heating, inhomogeneity of radiation capacity of the sample's surface and the inhomogeneity of the glue layer both by optimization of the control method and by processing of the obtained results, in particular, using the algorithm of differential filtration.

As a result of application of the proposed methods, we managed to decrease the level of interferences, connected to the nonuniformity of heating, to 0,7 °C (instead of 1,4 °C), to decrease the interference, caused by the nonuniformity of radiation activity, to 0,6 °C (instead of 2 °C) and to decrease temperature contrast, caused by the inhomogeneity of the glue layer, to 0,2 °C (instead of 1,2 °C). Due to this, the sensitivity of thermal flaw detection to identifying the flaws of the "adhesion failure" type in the honeycomb structures increased – dimension of threshold defect from 6 mm to 3 mm, and reliability of their detection increased by 17–20 %.

In the work we obtained new, scientifically substantiated, theoretical and experimental results, which in total are the solution to the practical scientific problem of optimization of procedure of the thermal flaw detection of honeycomb constructions by increasing the accuracy of function of interferences to the objects of aerospace sector of engineering.

### 8. Conclusions

1. There was developed a thermophysical model of OC, which, in comparison with the analogs, more fully reflects actual conditions of conducting the thermal flaw detection of honeycomb constructions. In particular, the interferences, caused by the inhomogeneity of internal structure, are included in the model. This makes it possible to evaluate the expected magnitude of signal from a flaw with higher reliability.

2. We proposed the procedure of optimization of the regime of conducting thermal flaw detection, based on the criterion of maximization of the ratio  $\Delta T_{def}/\Delta U$ , not the ratio  $\Delta T_{def}/\Delta T_e$ , which makes it possible to extend the limits of this method's applicability for the case of existence of several radiation interferences.

3. The method of dealing with the interference, caused by the inhomogeneity of the glue layer, by processing the obtained results by the algorithm of differential filtration, was proposed.

### References

1. Storozhenko, V. A. Termografiya v diagnostike i nerazrushayushchem kontrole [Text] / V. A. Storozhenko, V. A. Maslova. – Kharkiv: «Smit», 2004. – 160 p.

2. Maldague, X. P. Theory and Practice of Infrared Technology for Nondestructive Testing [Text] / X. P. Maldague. – John Wiley & Sons, Inc., 2001. – 684 p.
3. Vavilov, V. P. Infrakrasnaya termografiya i teplovoj kontrol' [Text] / V. P. Vavilov. – Moscow: ID Spektr, 2009. – 544 p.
4. Lykov, A. V. Teoriya teploprovodnosti [Text] / A. V. Lykov. – Moscow: Vysshaya shkola, 1967. – 602 p.
5. Storozhenko, V. A. Optimizaciya rezhimov teplovoj defektoskopii na osnove teplofizicheskogo modelirovaniya [Text] / V. A. Storozhenko, S. B. Malik, A. V. Myagkij // Visnik Nacional'nogo tekhnichnogo universitetu «Harkivs'kij politekhnichnij institut». Zbirnik naukovih prac'. Tematichnij vipusk: Priladi i metodi nerujnivnogo kontrolyu. – 2008. – Vol. 48. – P. 84–91.
6. Storozhenko, V. A. Optimizaciya procedury teplovoj defektoskopii sotovyh konstrukcij [Text] / V. A. Storozhenko, S. B. Malik, A. V. Myagkij, V. G. Tihij // TD i NK. – 2013. – Vol. 3. – P. 31–35.
7. Storozhenko, V. A. Primenenie termograficheskogo metoda kontrolyu dlya opredeleniya sodержaniya zhidkoj fazy v gazoprovodah [Text] / V. A. Storozhenko, S. N. Meshkov, S. A. Saprykin, A. V. Myagkij // Naukovo-tekhnichnij zhurnal «Metodi ta priladi kontrolyu yakosti». – 2009. – Vol. 22. – P. 117.
8. Vavilov, V. P. Teplovoj kontrol' korrozii v alyuminievyh panelyah samoletov [Text] / V. P. Vavilov, Guo Sin'yan', V. V. SHiryayev, D. A. Nesteruk // Defektoskopiya. – 2008. – Vol. 4. – P. 48–57.
9. Vavilov, V. P. Metody i ehksperimental'naya realizaciya impul'snogo teplovogo kontrolyu plazmennyyh pokrytij [Text] / V. P. Vavilov, A. I. Ivanov, D. A. Nesteruk, V. V. SHiryayev // Izvestiya TPU/TPU. – 2010 – Vol. 317, Issue 4. – P. 5–9.
10. Obbadi, A. Characterization of delamination by a thermal method of non destructive testing [Text] / A. Obbadi, S. Belattar // Proc. Vth International Workshop, Advances in Signal Processing for Non Destructive Evaluation of Materials, 2005. – P. 203–208.
11. Mallat, S. A Wavelet Tour of Signal Processing. The Sparse Way [Text] / S. Mallat. – N. Y.: Academic Press, 2008. – 805 p.
12. Yella, S. Artificial intelligence techniques for the automatic interpretation of data from non-destructive testing [Text] / S. Yella, M. S. Dougherty, N. K. Gupta // Insight. – 2006. – Vol. 48, Issue 1. – P. 10–20. doi: 10.1784/insi.2006.48.1.10
13. Fominceva, Yu. V. Realizaciya metoda teplovyh voln v teplovom kontrole izdelij iz kompozitov [Text] / Yu. V. Fominceva, D. A. Nesteruk // Vestnik nauk Sibiri. – 2014. – Vol. 2, Issue 12. – P. 235.
14. Bazhenov, B. N. Metod teplovogo kontrolyu lopatok turbin s ispol'zovaniem teplovoj volny [Text] / B. N. Bazhenov, S. I. Mel'nik, A. G. CHumakov // Aviacionno-kosmicheskaya tekhnika i tekhnologiya. – 2007. – Vol. 9, Issue 45. – P. 97–100.
15. Potapov, A. I. Vyyavlenie rassloenij i glubiny ih zaleganiya v ugleplastikovyyh konstrukciyah s ispol'zovaniem vihretokovogo vida nerazrushayushchego kontrolyu [Text] / A. I. Potapov, V. A. Syas'ko, D. N. Chertov // Izvestiya vysshih uchebnyh zavedenij. – 2012. – Vol. 8. – P. 66–69.
16. Maldague, X. P. V. Fundamentals of Infrared and Thermal Testing. in Nondestructive Handbook, Infrared and Thermal Testing. Vol. 3 [Text] / X. P. V. Maldague, T. S. Jones, H. Kaplan, S. Marinetti, M. Prystay. – Columbus, Ohio, ASNT Press, 2001. – 718 p.
17. Storozhenko, V. A. Obrabotka rezul'tatov teplovoj defektoskopii sotovyh konstrukcij s cel'yu ponizhe-niya urovnya pomekh [Text] / V. A. Storozhenko, O. V. Lazorenko, A. V. Myagkij // Visnik NTU «HPI». Seriya: Elektroenergetika ta peretvoryuval'na tekhnika. – 2013. – Vol. 34, Issue 1007. – P. 108–112.